Supplement of Hydrol. Earth Syst. Sci., 27, 4579–4593, 2023
https://doi.org/10.5194/hess-27-4579-2023-supplement

Hydrology and Earth System Sciences
Open Access
EGU

Supplement of

Prediction of absolute unsaturated hydraulic conductivity – comparison of four different capillary bundle models

Andre Peters et al.

Correspondence to: Andre Peters (a.peters@tu-braunschweig.de)

S 1.1: All calibration curves (pages 2 to 13)

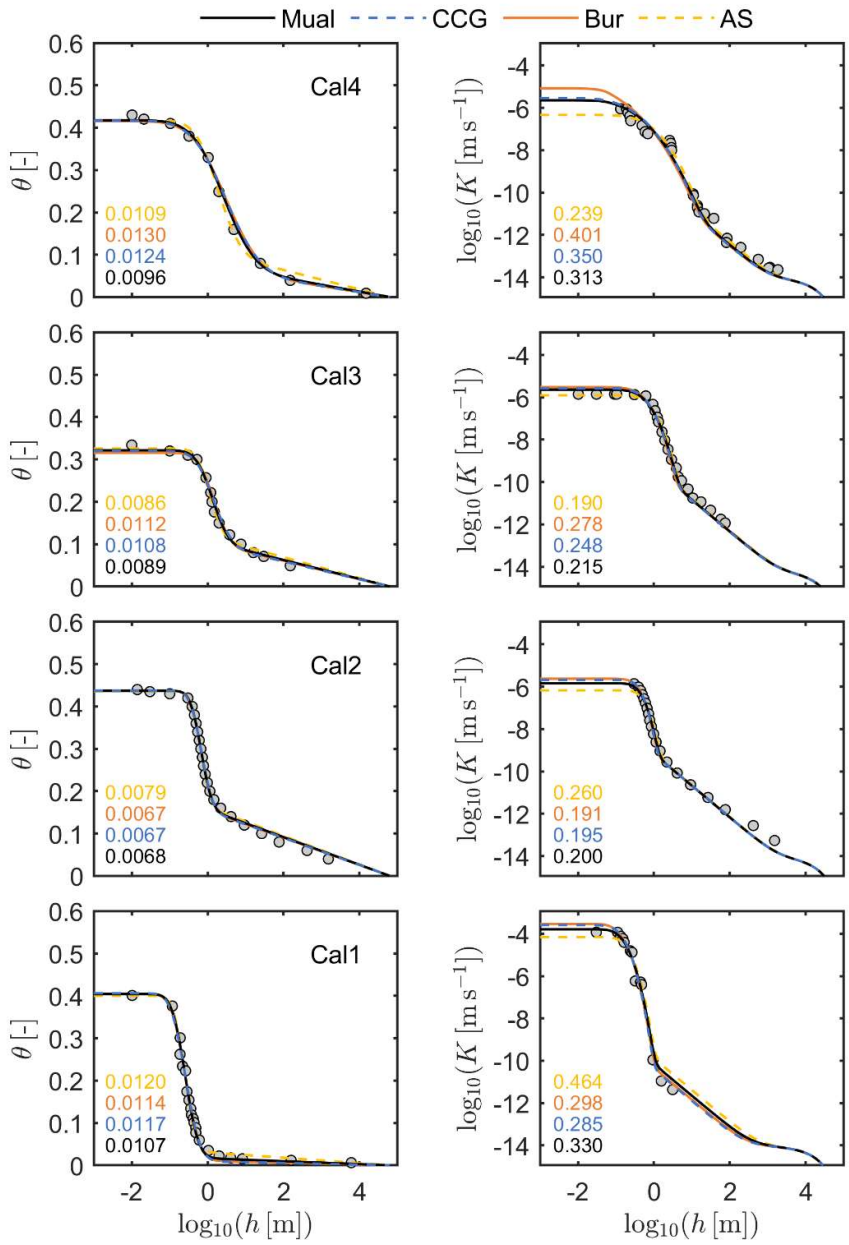

Fig. S1: Calibration data sets and the fitted water retention and conductivity functions used to calibrate the saturated tortuosity coefficient τ_s. Shown are data set 1 to 4 of the 12 calibration data sets and the **Kos-PDI** retention model combined with the 4 capillary bundle models. Parameter τ_s and the retention parameters were allowed to vary. Numbers in the subplots indicate $RMSE_\theta$ and $RMSE_{logK}$ values for the various model combinations.

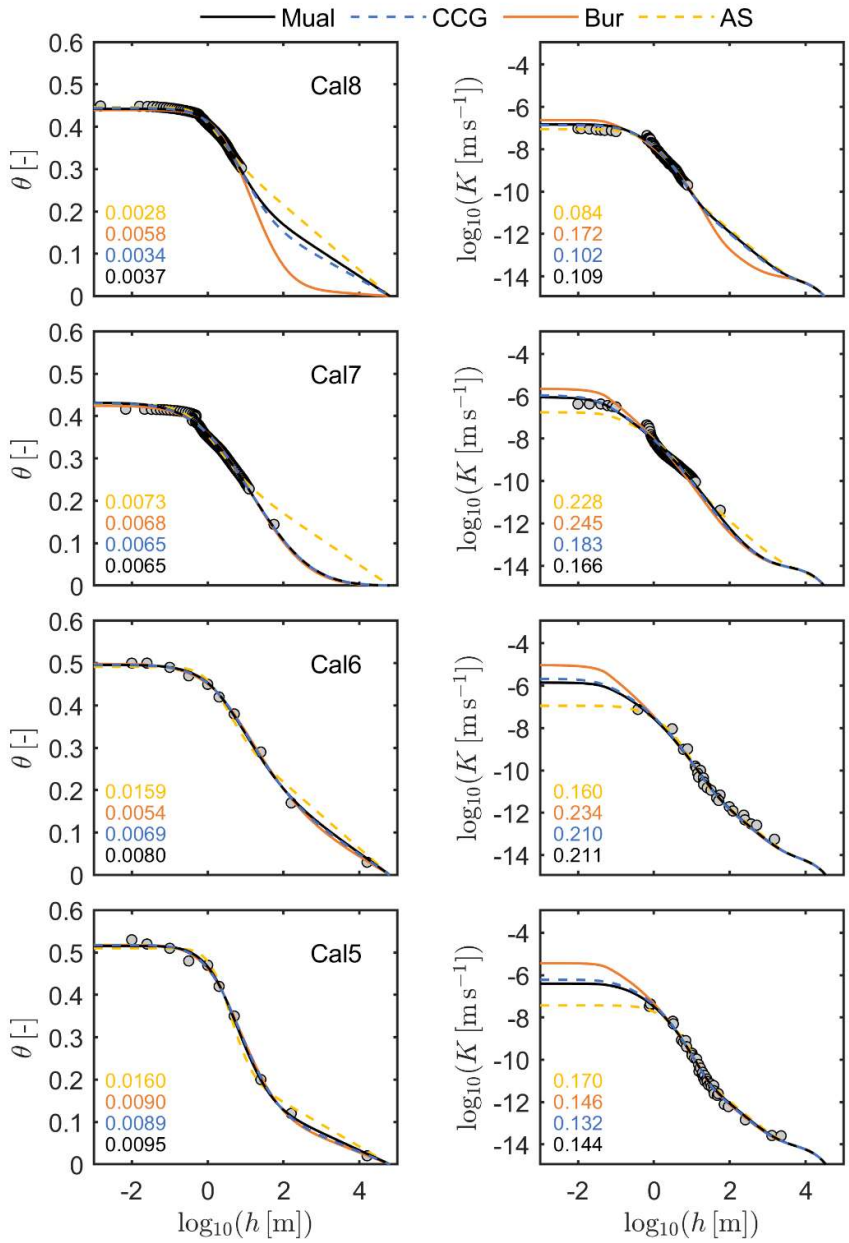

17

18 Fig. S2: Calibration data sets and the fitted water retention and conductivity functions used to
19 calibrate the saturated tortuosity coefficient τ_s. Shown are data set 5 to 8 of the 12 calibration data
20 sets and the **Kos-PDI** retention model combined with the 4 capillary bundle models. Parameter τ_s
21 and the retention parameters were allowed to vary. Numbers in the subplots indicate $RMSE_\theta$ and
22 $RMSE_{logK}$ values for the various model combinations.

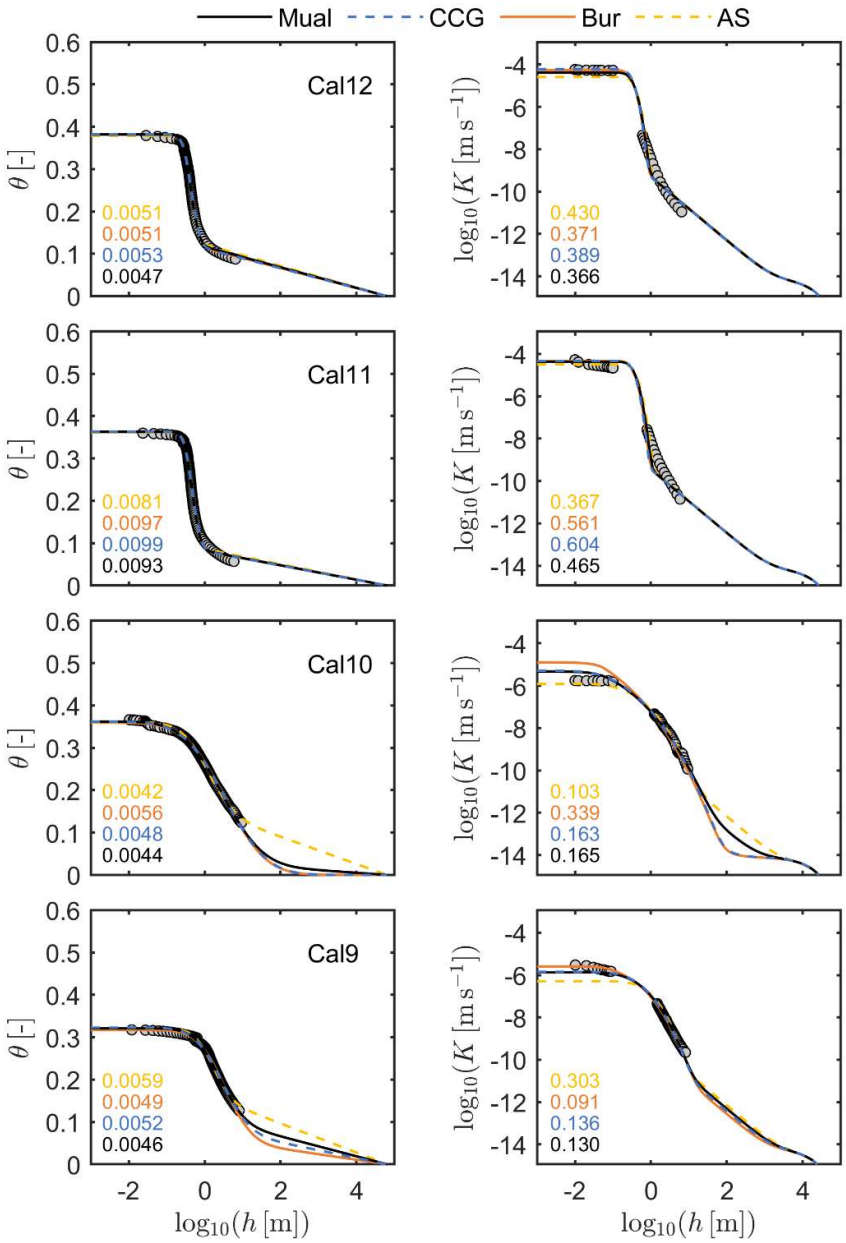

23

24 Fig. S3: Calibration data sets and the fitted water retention and conductivity functions used to
25 calibrate the saturated tortuosity coefficient τ_s. Shown are data set 9 to 12 of the 12 calibration data
26 sets and the **Kos-PDI** retention model combined with the 4 capillary bundle models. Parameter τ_s
27 and the retention parameters were allowed to vary. Numbers in the subplots indicate $RMSE_\theta$ and
28 $RMSE_{logK}$ values for the various model combinations.

29

30

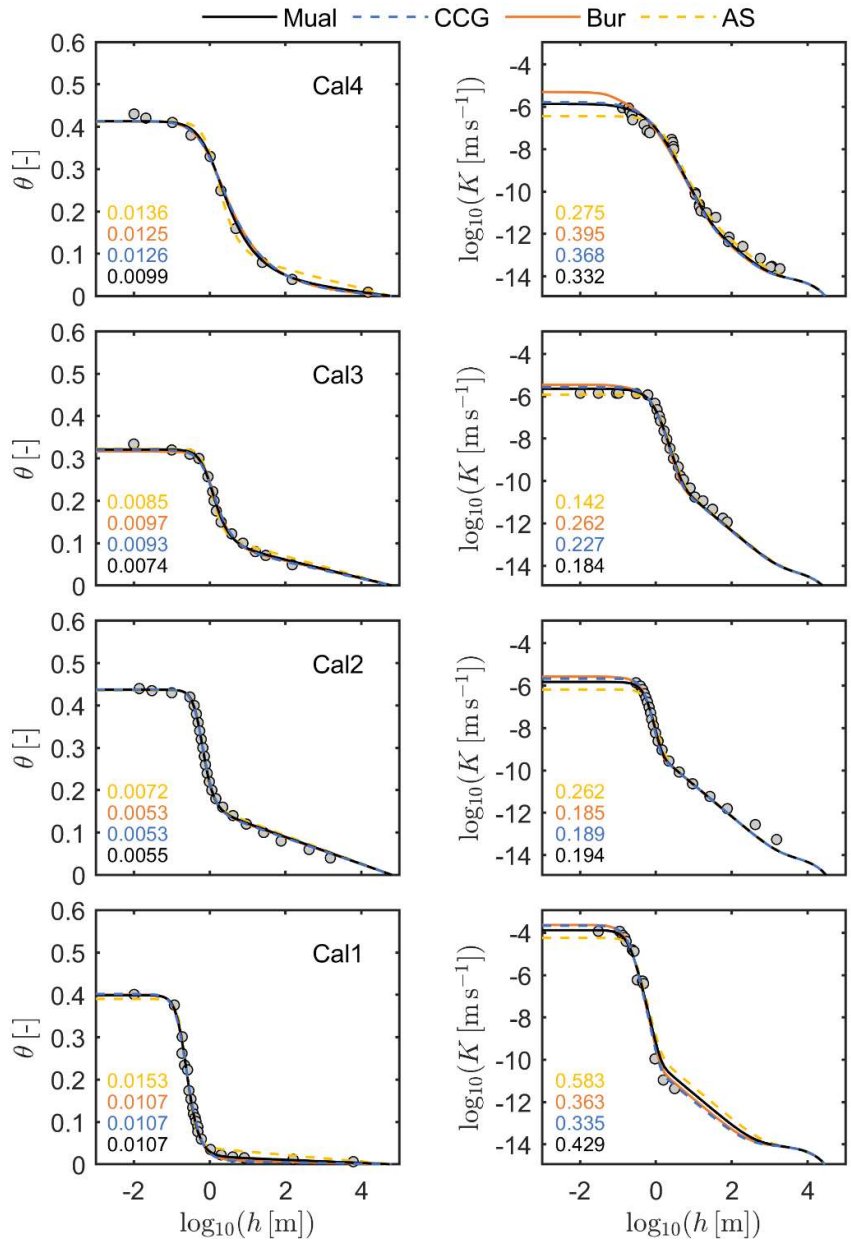

31

32 Fig. S4: Calibration data sets and the fitted water retention and conductivity functions used to
33 calibrate the saturated tortuosity coefficient τ_s. Shown are data set 1 to 4 of the 12 calibration data
34 sets and the **vGc-PDI** retention model combined with the 4 capillary bundle models. Parameter τ_s
35 and the retention parameters were allowed to vary. Numbers in the subplots indicate $RMSE_\theta$ and
36 $RMSE_{logK}$ values for the various model combinations.

37

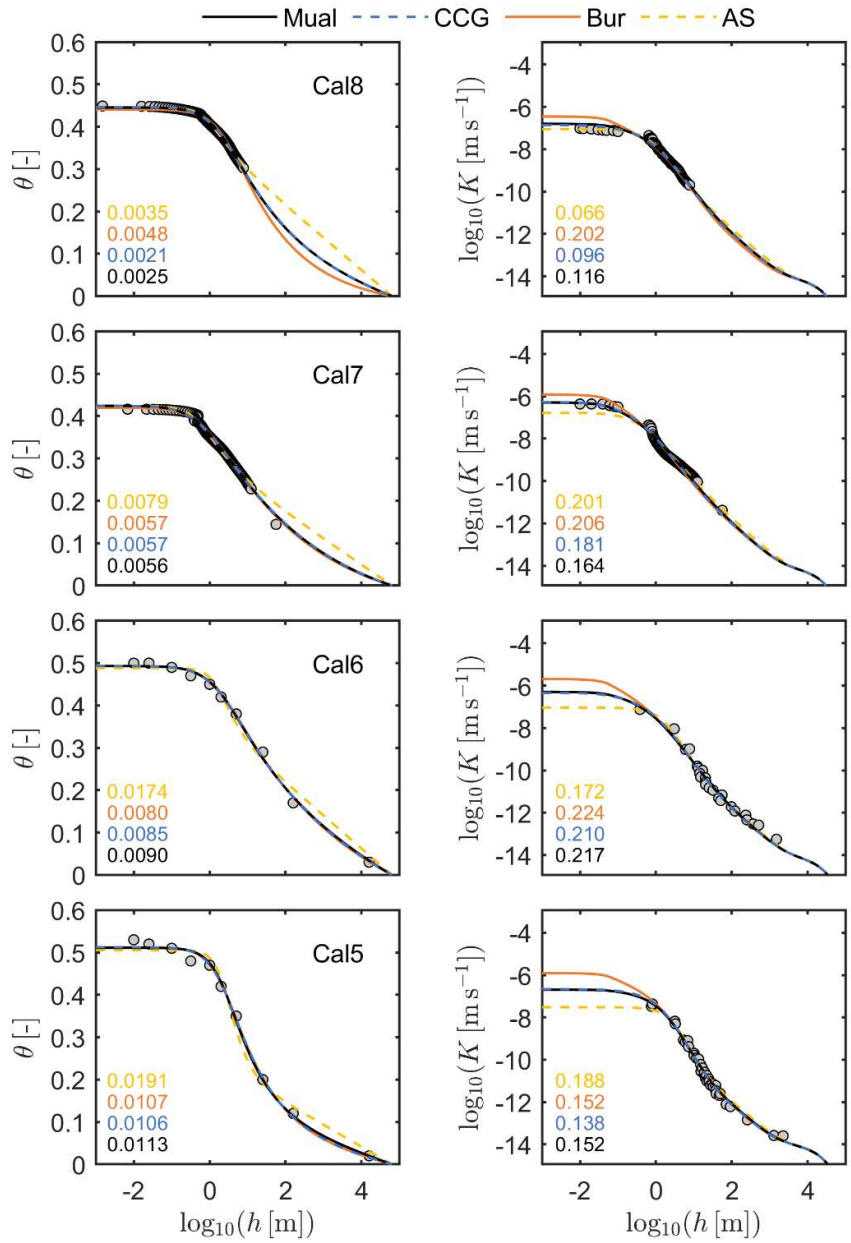

38

39 Fig. S5: Calibration data sets and the fitted water retention and conductivity functions used to
40 calibrate the saturated tortuosity coefficient τ_s. Shown are data set 5 to 8 of the 12 calibration data
41 sets and the **vGc-PDI** retention model combined with the 4 capillary bundle models. Parameter τ_s
42 and the retention parameters were allowed to vary. Numbers in the subplots indicate $RMSE_\theta$ and
43 $RMSE_{logK}$ values for the various model combinations.

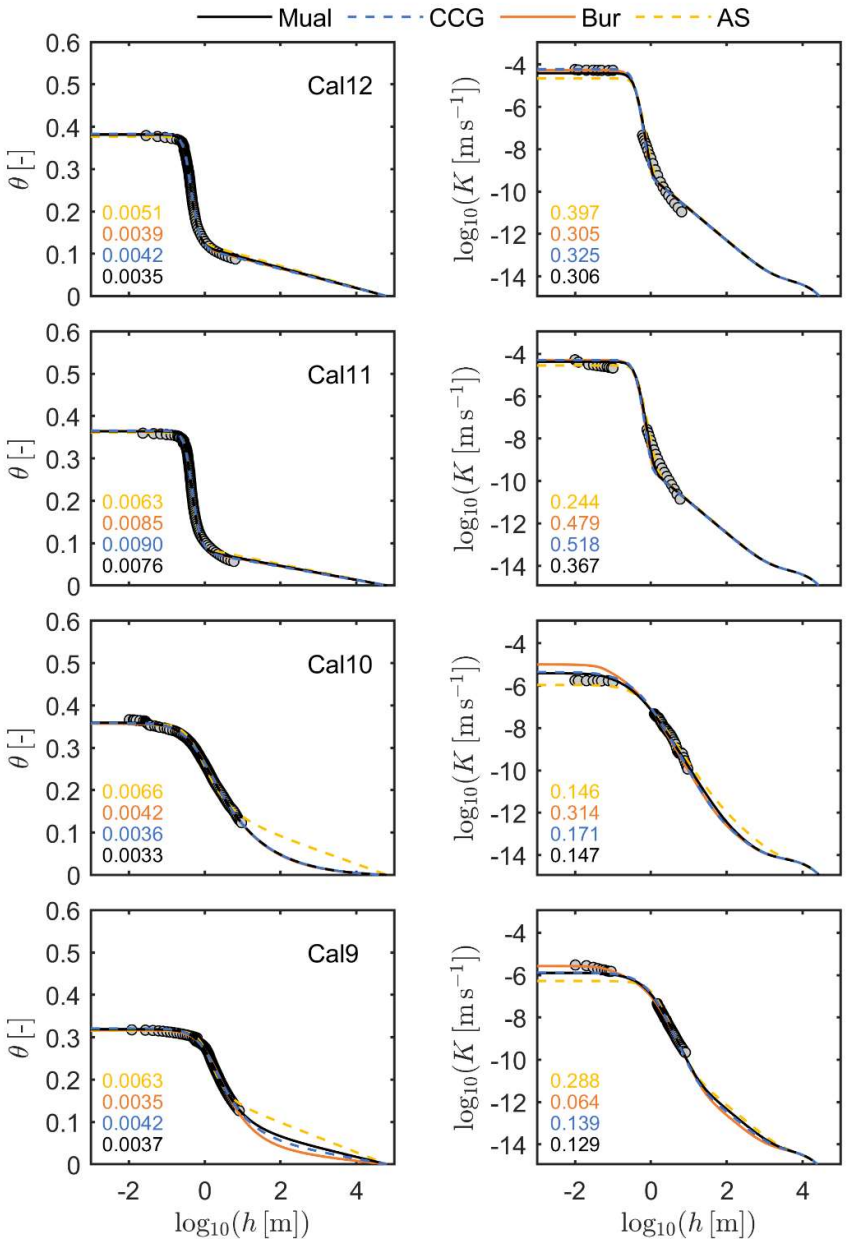

Fig. S6 Calibration data sets and the fitted water retention and conductivity functions used to calibrate the saturated tortuosity coefficient τ_s. Shown are data set 9 to 12 of the 12 calibration data sets and the **vGc-PDI** retention model combined with the 4 capillary bundle models. Parameter τ_s and the retention parameters were allowed to vary. Numbers in the subplots indicate $RMSE_\theta$ and $RMSE_{logK}$ values for the various model combinations.

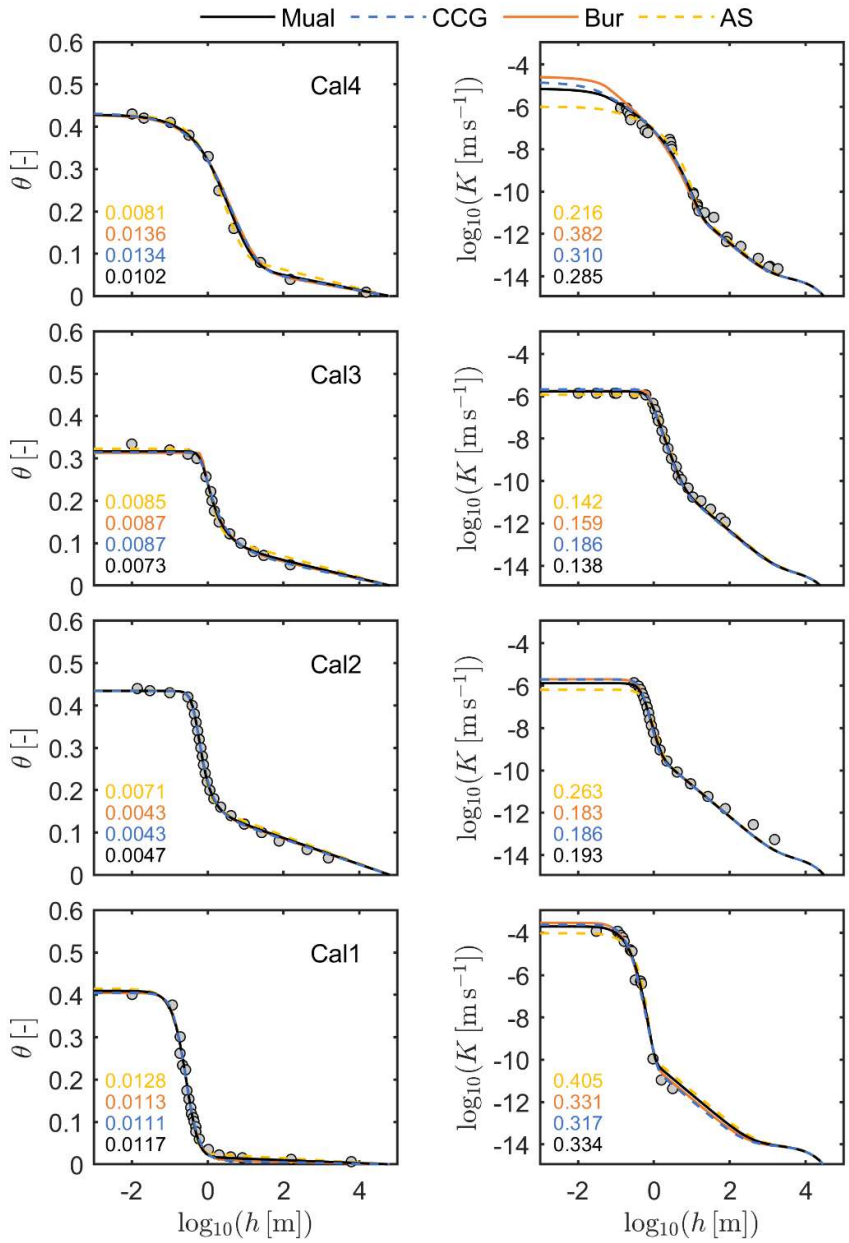

51

52 Fig. S7: Calibration data sets and the fitted water retention and conductivity functions used to
53 calibrate the saturated tortuosity coefficient τ_s. Shown are data set 1 to 4 of the 12 calibration data
54 sets and the **vGmn-PDI** retention model combined with the 4 capillary bundle models. Parameter τ_s
55 and the retention parameters were allowed to vary. Numbers in the subplots indicate $RMSE_\theta$ and
56 $RMSE_{logK}$ values for the various model combinations.

57

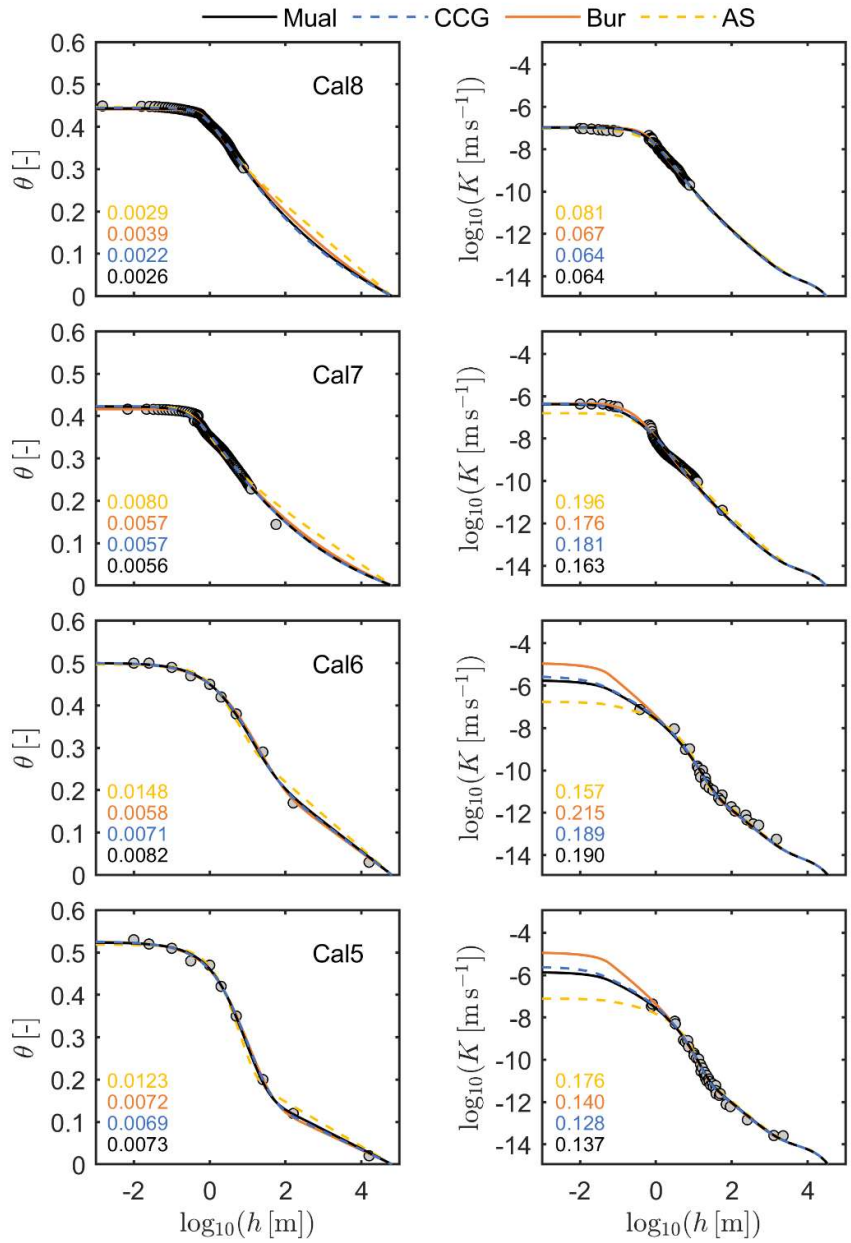

58

59 Fig. S8: Calibration data sets and the fitted water retention and conductivity functions used to
60 calibrate the saturated tortuosity coefficient τ_s. Shown are data set 5 to 8 of the 12 calibration data
61 sets and the **vGmn-PDI** retention model combined with the 4 capillary bundle models. Parameter τ_s
62 and the retention parameters were allowed to vary. Numbers in the subplots indicate $RMSE_\theta$ and
63 $RMSE_{logK}$ values for the various model combinations.

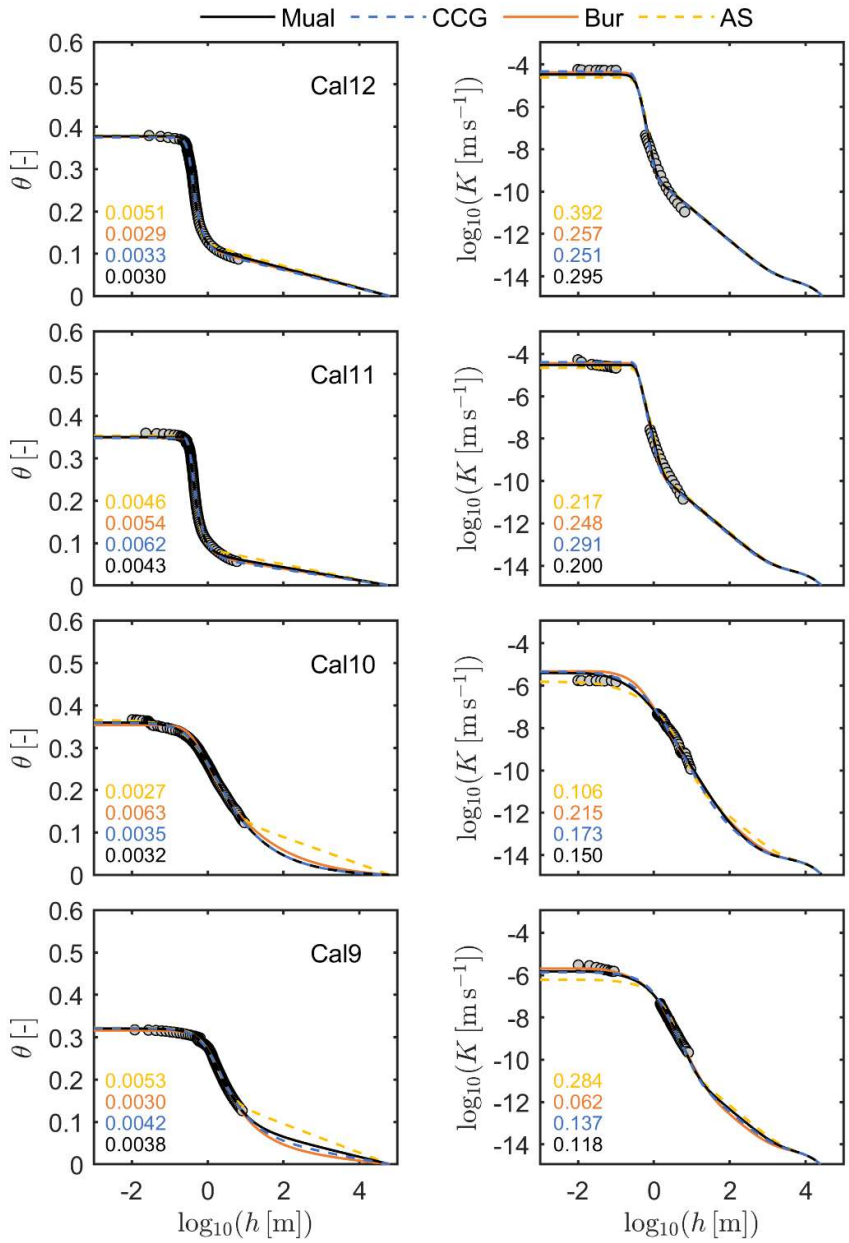

64

65 Fig. S9: Calibration data sets and the fitted water retention and conductivity functions used to
66 calibrate the saturated tortuosity coefficient τ_s. Shown are data set 9 to 12 of the 12 calibration data
67 sets and the **vGmn-PDI** retention model combined with the 4 capillary bundle models. Parameter τ_s
68 and the retention parameters were allowed to vary. Numbers in the subplots indicate $RMSE_\theta$ and
69 $RMSE_{logK}$ values for the various model combinations.

70

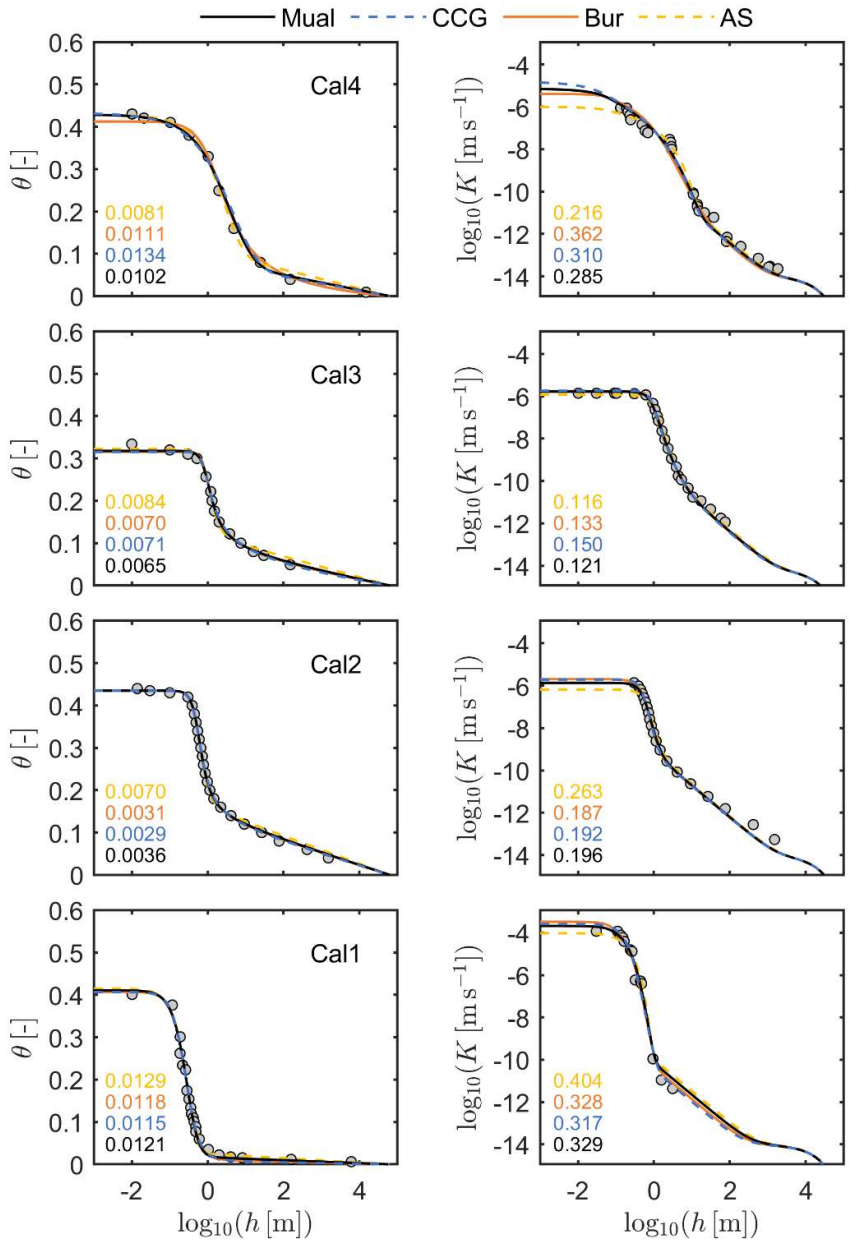

71

72 Fig. S10: Calibration data sets and the fitted water retention and conductivity functions used to
73 calibrate the saturated tortuosity coefficient τ_s. Shown are data set 1 to 4 of the 12 calibration data
74 sets and the **FX-PDI** retention model combined with the 4 capillary bundle models. Parameter τ_s and
75 the retention parameters were allowed to vary. Numbers in the subplots indicate $RMSE_\theta$ and
76 $RMSE_{logK}$ values for the various model combinations.

77

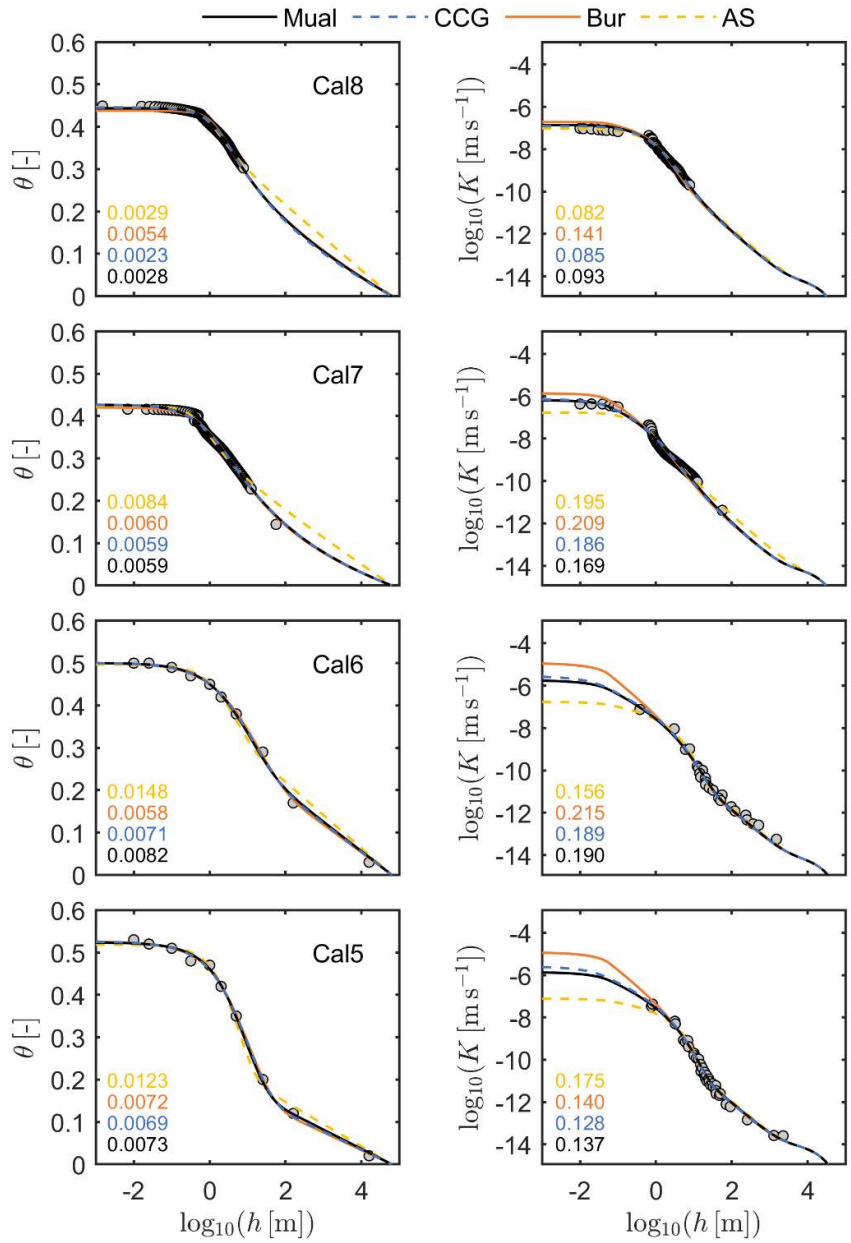

78

79 Fig. S11: Calibration data sets and the fitted water retention and conductivity functions used to
80 calibrate the saturated tortuosity coefficient τ_s. Shown are data set 5 to 8 of the 12 calibration data
81 sets and the **FX-PDI** retention model combined with the 4 capillary bundle models. Parameter τ_s and
82 the retention parameters were allowed to vary. Numbers in the subplots indicate $RMSE_\theta$ and
83 $RMSE_{logK}$ values for the various model combinations.

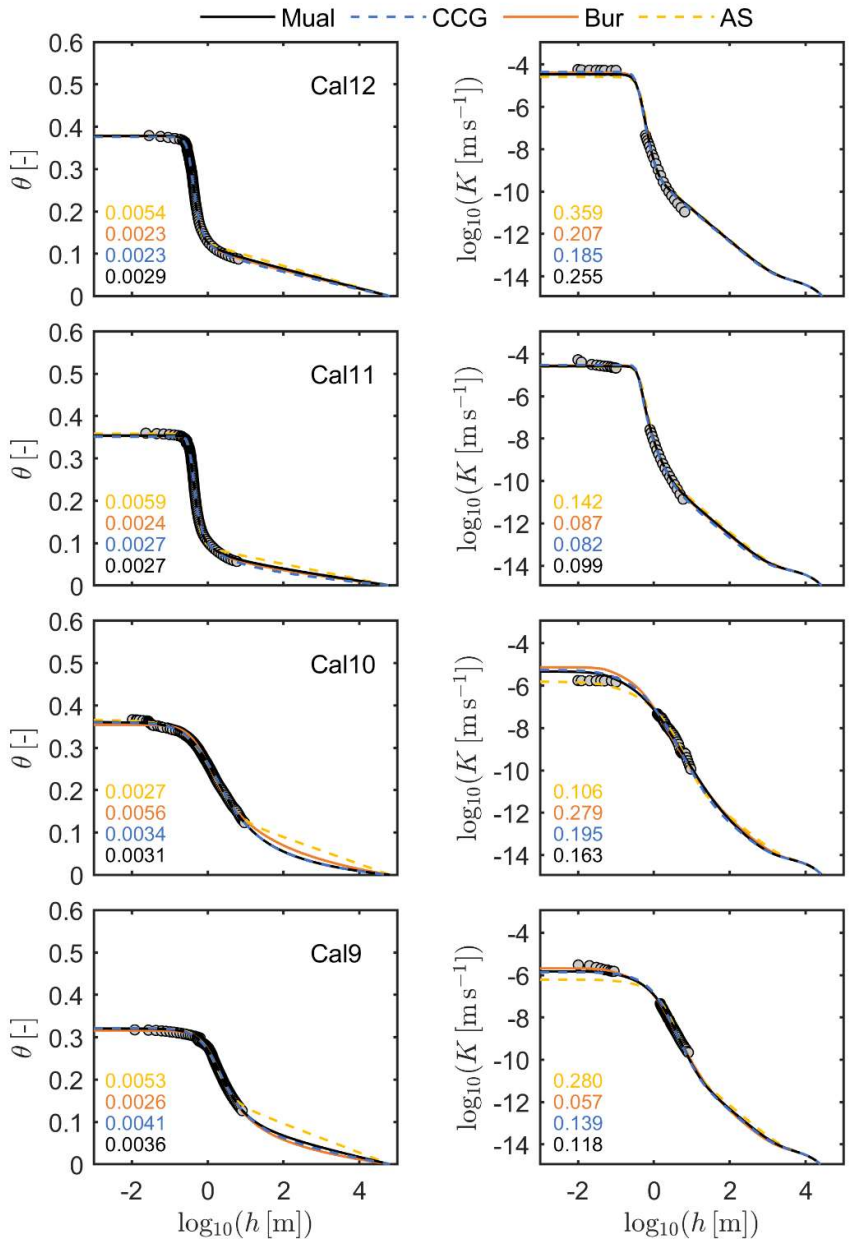

84

85 Fig. S12: Calibration data sets and the fitted water retention and conductivity functions used to
86 calibrate the saturated tortuosity coefficient τ_s. Shown are data set 9 to 12 of the 12 calibration data
87 sets and the **FX-PDI** retention model combined with the 4 capillary bundle models. Parameter τ_s and
88 the retention parameters were allowed to vary. Numbers in the subplots indicate $RMSE_\theta$ and
89 $RMSE_{logK}$ values for the various model combinations.

90

91

S 1.2: All validation curves (pages 14 to 21)

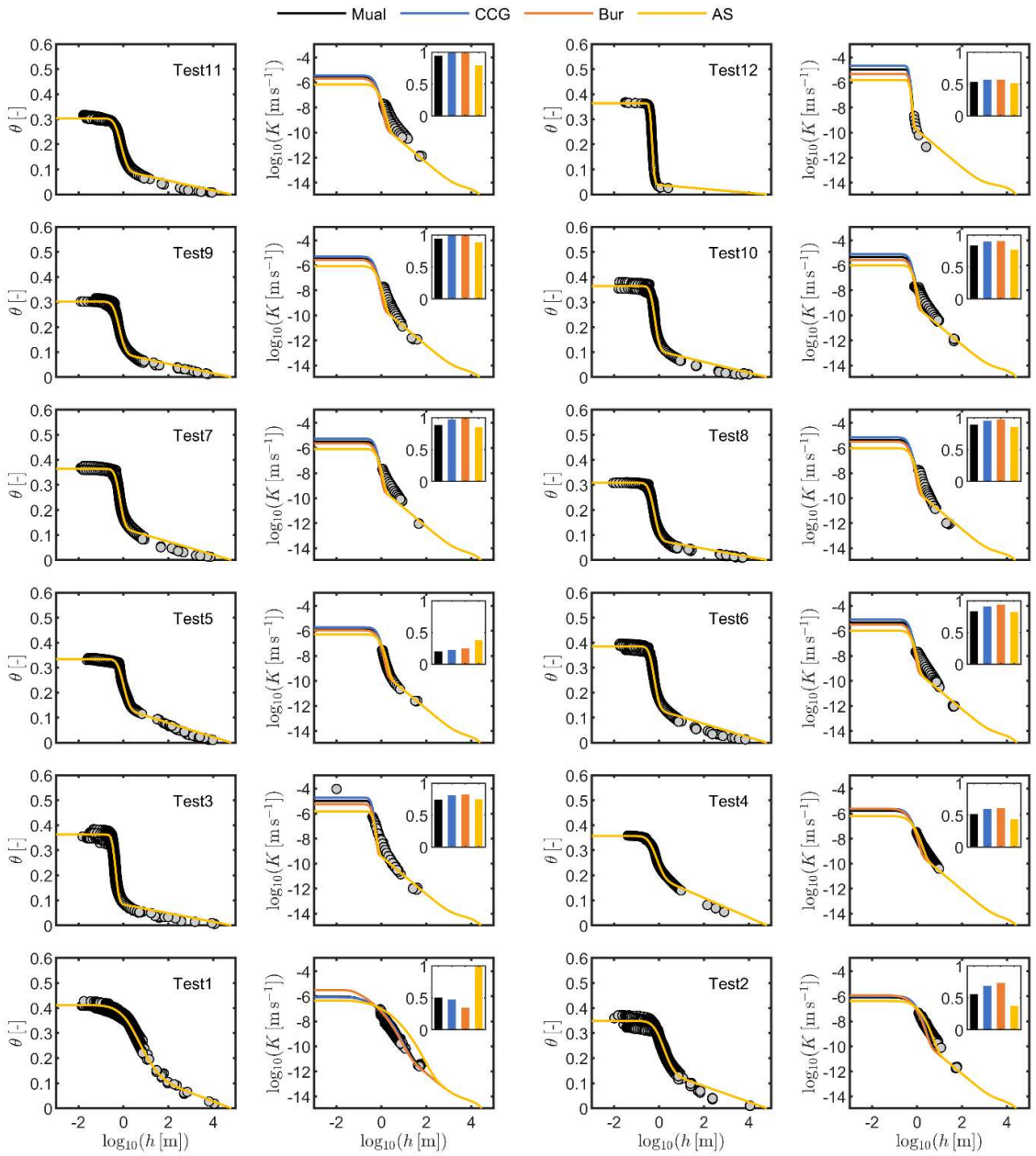

Fig. S13: Measured data (dots), fitted retention functions (left) and fully predicted conductivity functions (right). Shown are the first 12 out of the 23 test data sets and the **Kos-PDI** retention model combined with the 4 capillary bundle models. Bars show the $RMSE_{logK}$ values for the different used capillary bundle models. Note that the conductivity curves are not fits to the data but pure predictions.

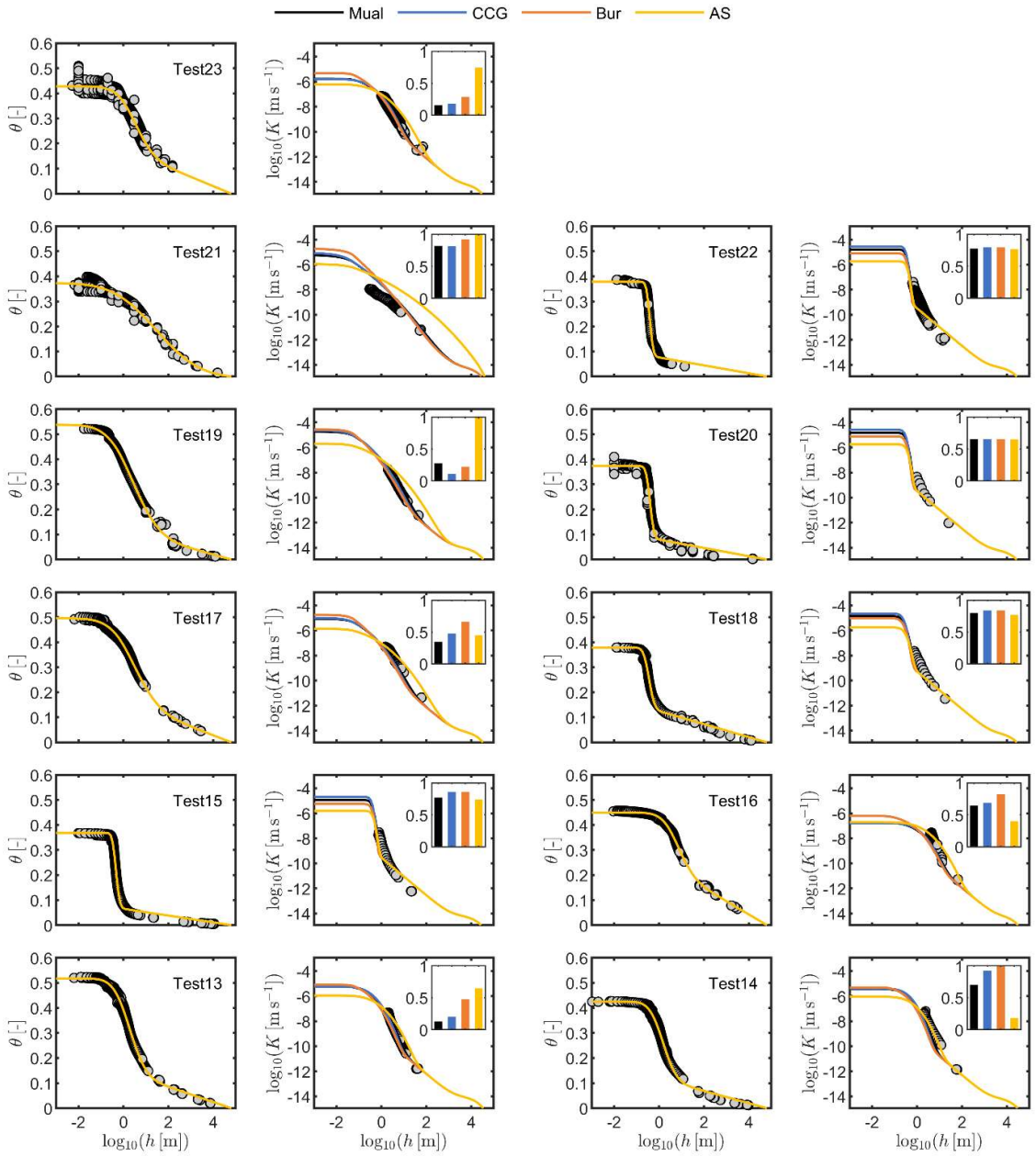

Fig. S14: Measured data (dots), fitted retention functions (left) and fully predicted conductivity functions (right). Shown are data set 13 to 23 of the test data sets and the **Kos-PDI** retention model combined with the 4 capillary bundle models. Bars show the $RMSE_{logK}$ values for the different used capillary bundle models. Note that the conductivity curves are not fits to the data but pure predictions.

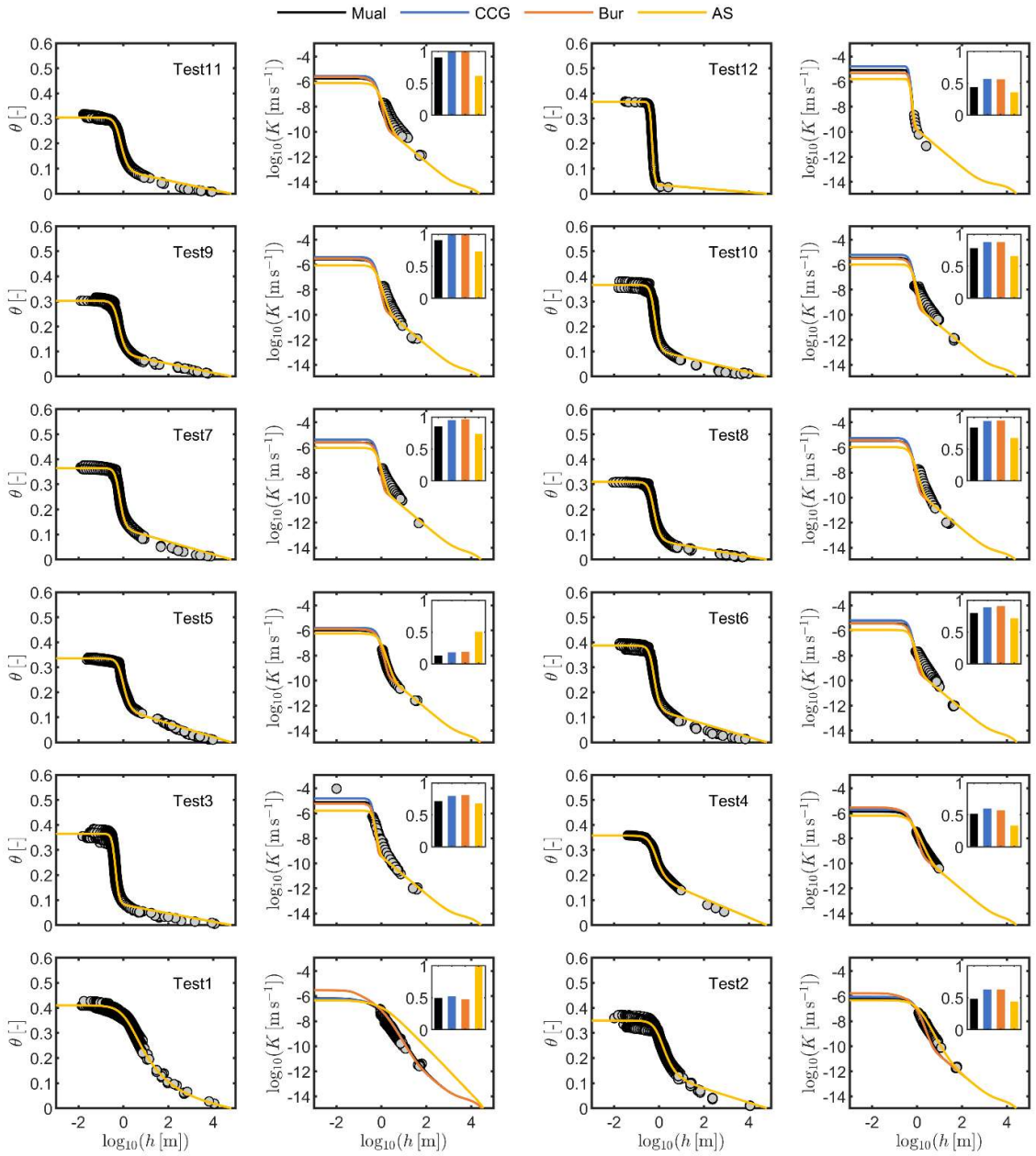

107

108 Fig. S15: Measured data (dots), fitted retention functions (left) and fully predicted conductivity
109 functions (right). Shown are the first 12 out of the 23 test data sets and the **vGc-PDI** retention model
110 combined with the 4 capillary bundle models. Bars show the $RMSE_{logK}$ values for the different used
111 capillary bundle models. Note that the conductivity curves are not fits to the data but pure
112 predictions.

113

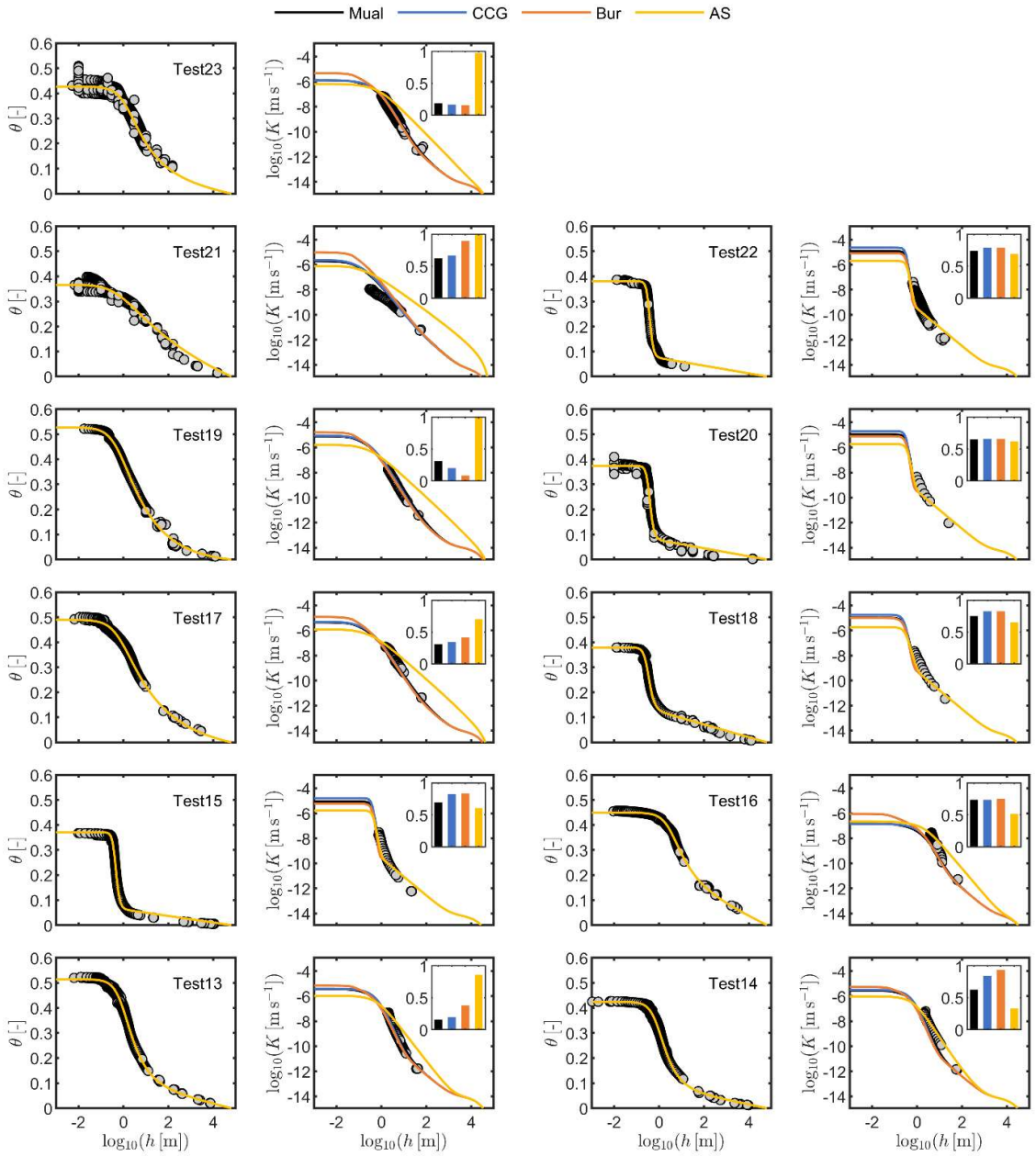

114

115 Fig. S16: Measured data (dots), fitted retention functions (left) and fully predicted conductivity
116 functions (right). Shown are data set 13 to 23 of the test data sets and the **vGc-PDI** retention model
117 combined with the 4 capillary bundle models. Bars show the $RMSE_{logK}$ values for the different used
118 capillary bundle models. Note that the conductivity curves are not fits to the data but pure
119 predictions.

120

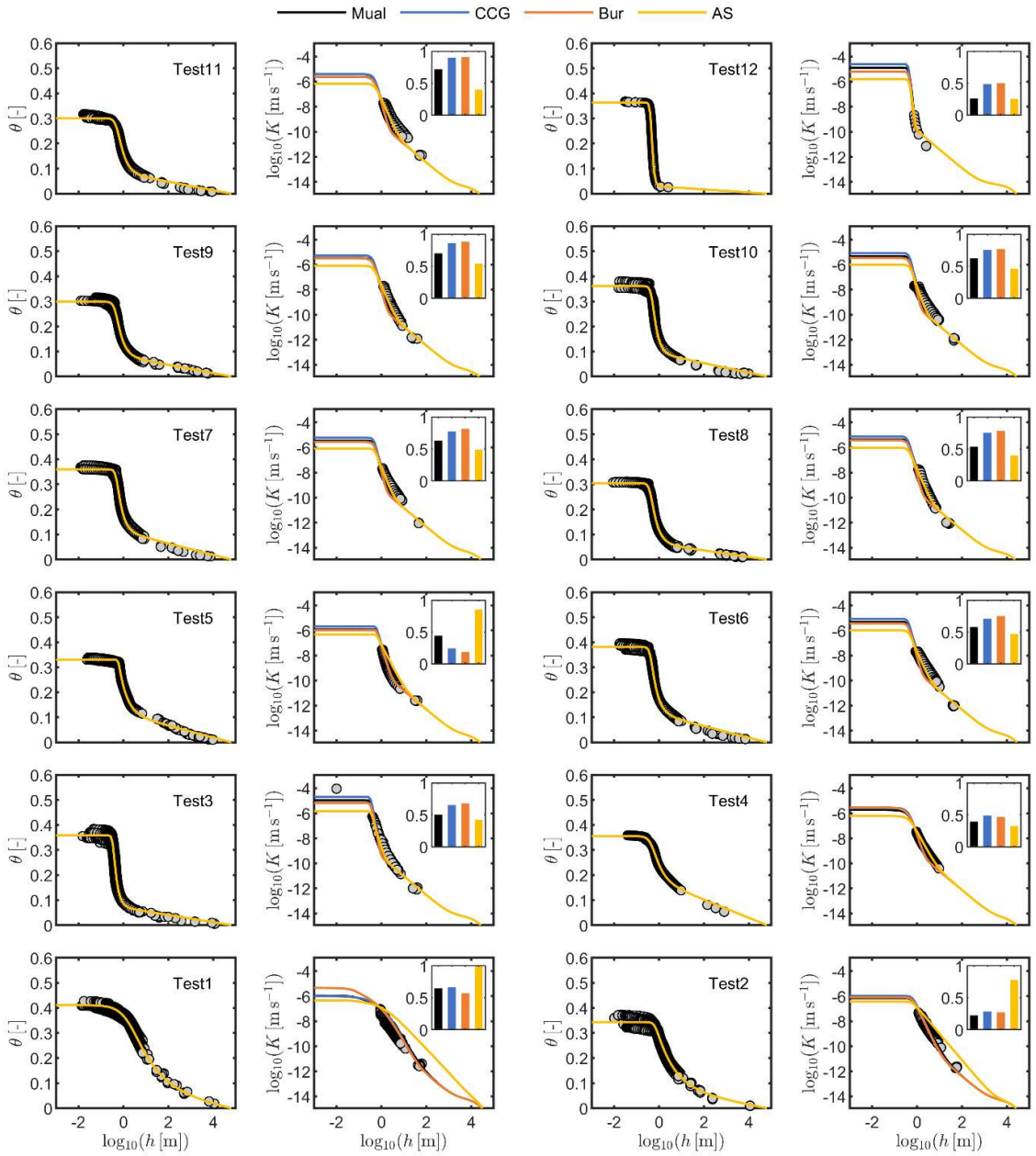

121

122 Fig. S17: Measured data (dots), fitted retention functions (left) and fully predicted conductivity
123 functions (right). Shown are the first 12 out of the 23 test data sets and the **vGmn-PDI** retention
124 model combined with the 4 capillary bundle models. Bars show the $RMSE_{logK}$ values for the different
125 used capillary bundle models. Note that the conductivity curves are not fits to the data but pure
126 predictions.

127

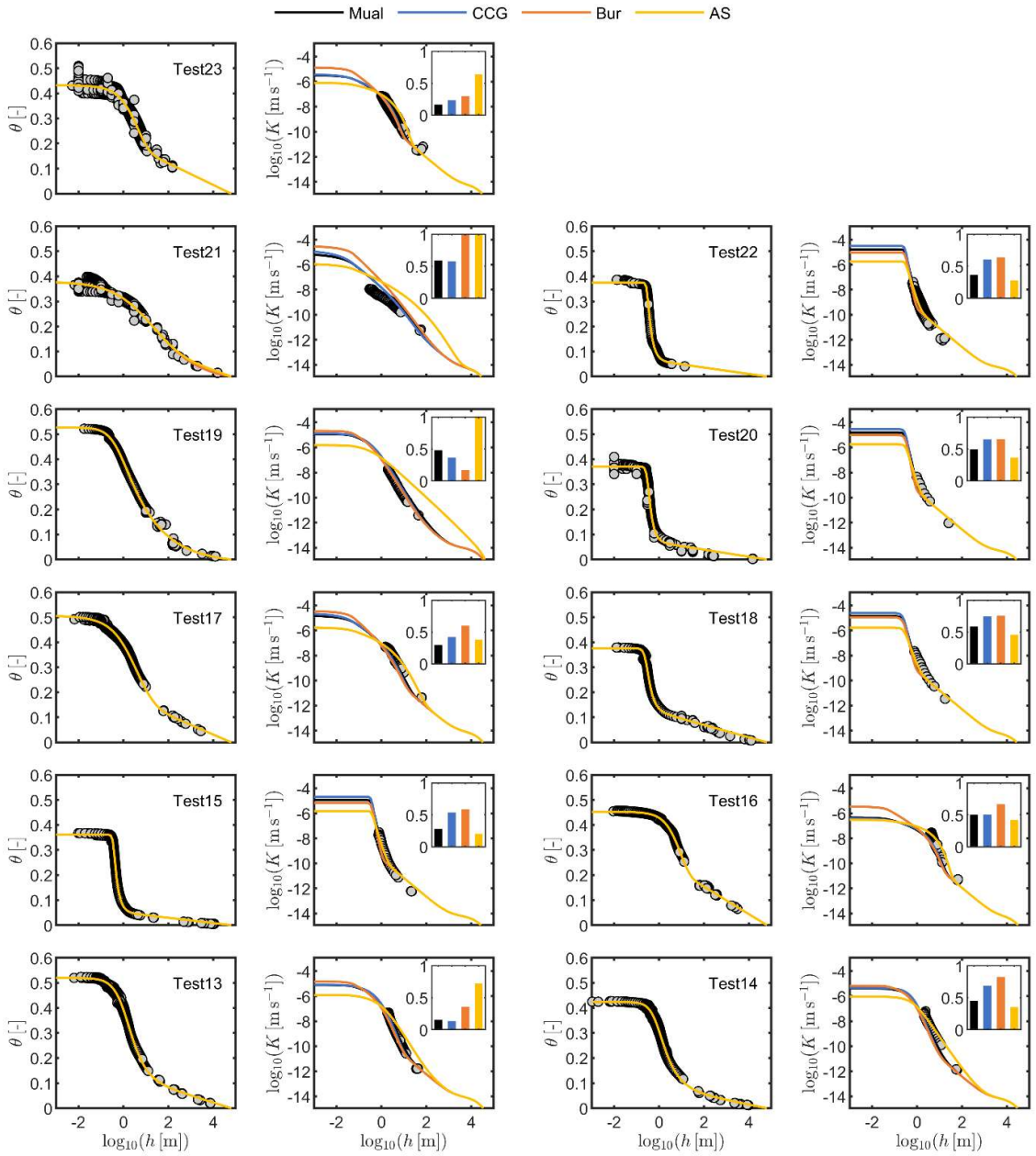

Fig. S18: Measured data (dots), fitted retention functions (left) and fully predicted conductivity functions (right). Shown are data set 13 to 23 of the test data sets and the **vGmn-PDI** retention model combined with the 4 capillary bundle models. Bars show the $RMSE_{logK}$ values for the different used capillary bundle models. Note that the conductivity curves are not fits to the data but pure predictions.

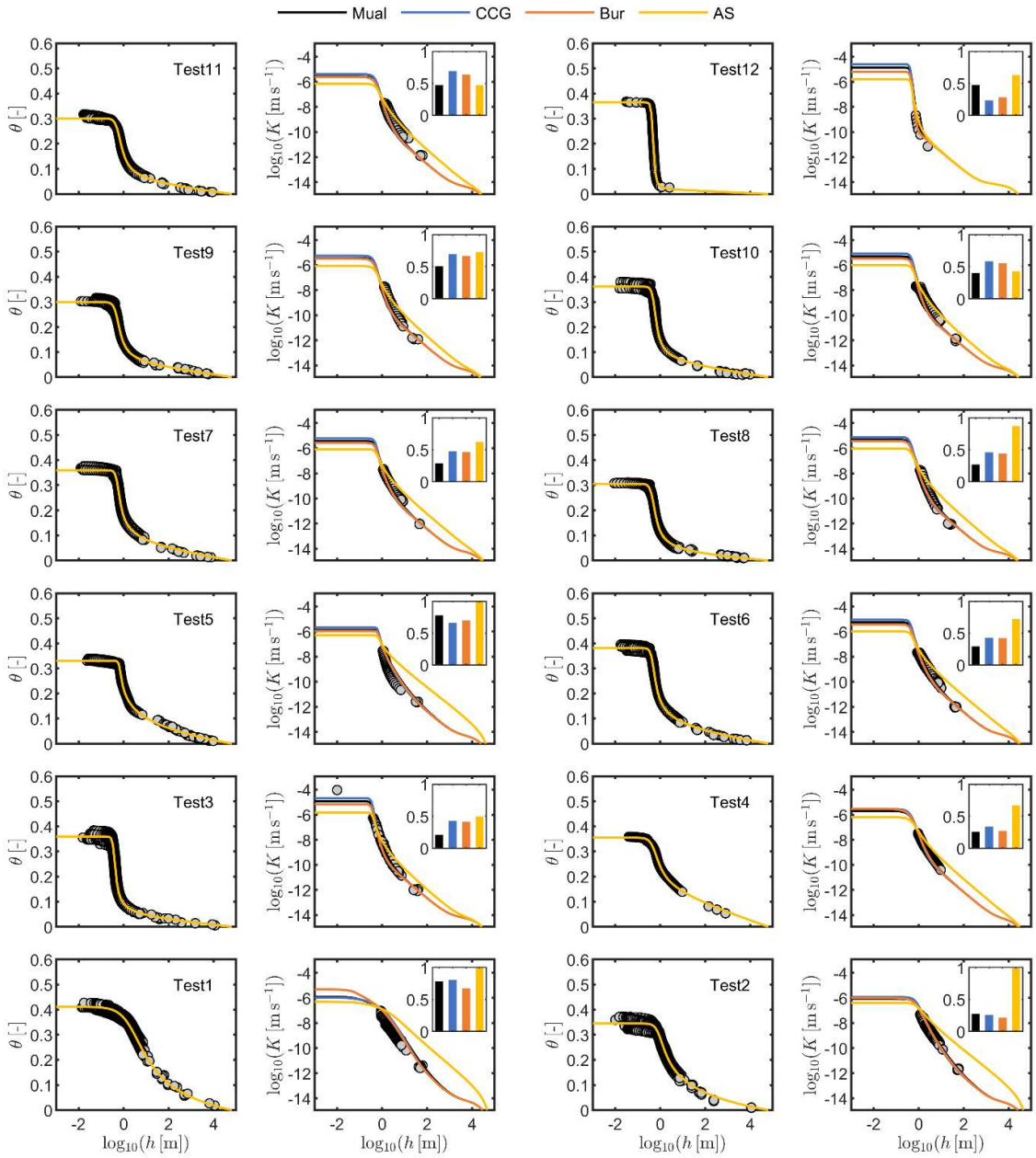

Fig. S19: Measured data (dots), fitted retention functions (left) and fully predicted conductivity functions (right). Shown are the first 12 out of the 23 test data sets and the **FX-PDI** retention model combined with the 4 capillary bundle models. Bars show the $RMSE_{logK}$ values for the different used capillary bundle models. Note that the conductivity curves are not fits to the data but pure predictions.

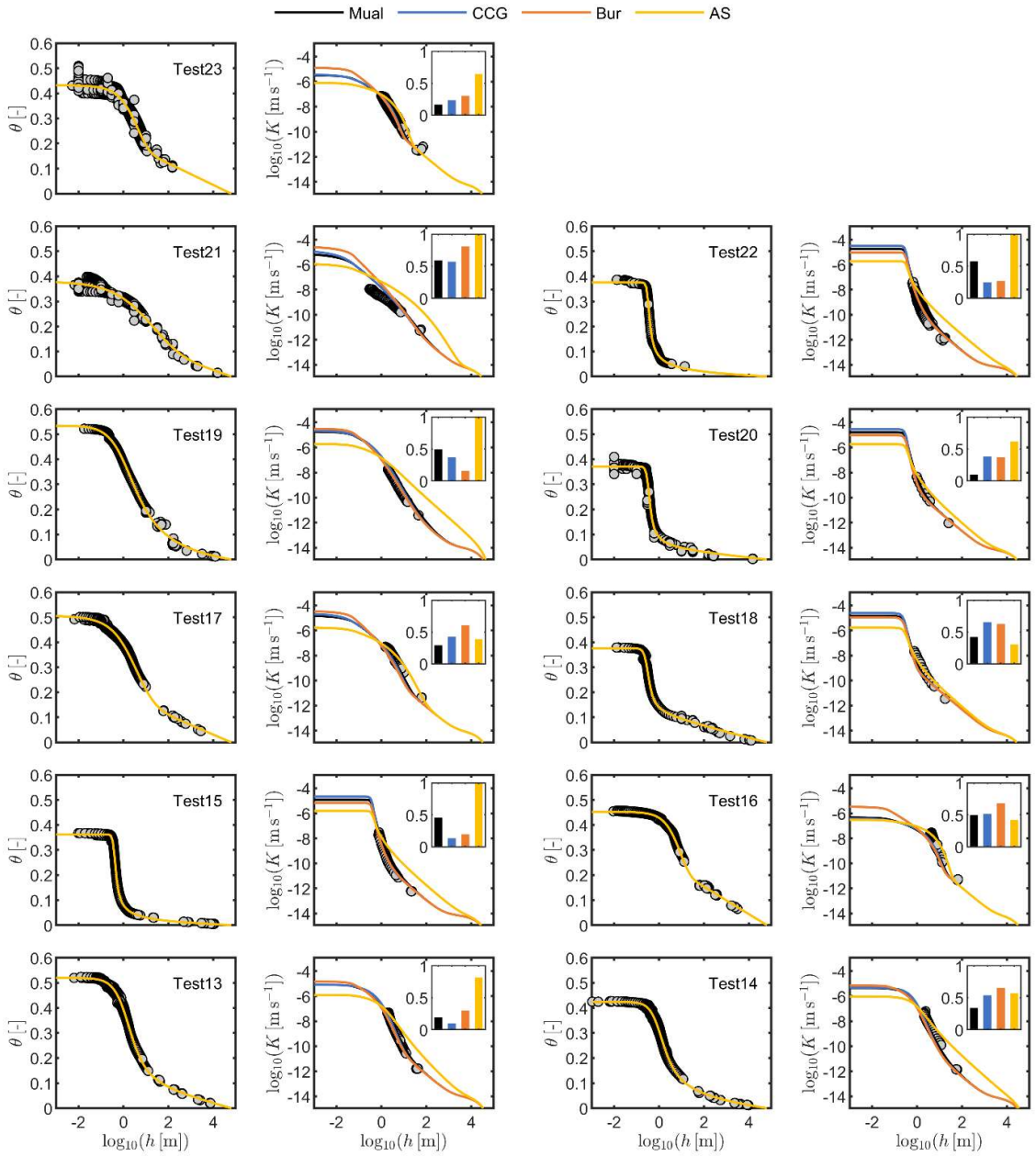

141

142 Fig. S20: Measured data (dots), fitted retention functions (left) and fully predicted conductivity
143 functions (right). Shown are data set 13 to 23 of the test data sets and the **FX-PDI** retention model
144 combined with the 4 capillary bundle models. Bars show the $RMSE_{logK}$ values for the different used
145 capillary bundle models. Note that the conductivity curves are not fits to the data but pure
146 predictions.

147